3D PRINTED MICRO LIQUID THERMAL REGULATOR (MLTR) FOR *IN-VIVO* CHRONIC PAIN APPLICATIONS

Jazune Madas[1], Andre Childs[1], Jichao Ma[1], Jin Chen[1], Lei Zhai[1], Zixi Jack Cheng[1]*, Swaminathan Rajaraman[1]**
[1]University of Central Florida, USA

ABSTRACT

The micro-liquid thermal regulator, or MLTR, is a novel 3D-printed implantable device for *in-vivo* thermoregulation tests. The efficient micro-manifold design within the device allows for minimal water pressure yet high liquid throughput, creating an efficient thermoregulation effect. Upon activation, the device demonstrates impressive capabilities, swiftly lowering surface temperatures from ambient room temperature of 25.3°C to 14.4°C. This capacity to achieve temperatures below 37°C, which is the physical norm, holds promise for influencing physiological processes associated with pain transmission. Future applications anticipate the implantation of the MLTR onto the dorsal root ganglia for comprehensive testing, furthering its potential in advancing research and therapeutics.

KEYWORDS

3D Printing, Gut Pain, Microfluidics, Thermoregulation, Implant

INTRODUCTION

According to a survey conducted by the National Center for Health Statistics (NCHS), a significant portion, approximately 20%, of American adults suffer from chronic pain **[1]**. Furthermore, 8% of these individuals experience high-impact chronic pain in the spine, gut, hands, and feet, which significantly affects their quality of life. Inflammation and pain serve as vital indicators of underlying issues within the body and the initiation of the body's healing process **[2]**. It is also known that chronic and emotional stress can lead to the development of visceral gut pain (VGP) in the form of irritable bowel syndrome (IBS) **[3]**. Chronic visceral gut pain affects individuals the most due to the gut brain axis. There is data to show that individuals who suffer from gastrointestinal disorders have an increased chance of developing depression and anxiety **[4]**. Currently there are only limited options to treat VGP such as low fermentable oligosaccharides, disaccharides, monosaccharides, and polyols (FODMAP) diet, physical and mental therapy, as well as opoids, which can lead to opioid dependency, and negatively impact mental health. The limited availability of safe non-opioid pain therapies highlights the need for alternative approaches. One potential alternative therapy for pain management involves the application of local cooling and knowledge of pains gate control theory **[5]**. When a body system temperature is reduced below the normal range of 37°C, physiological processes within that system are disrupted **[5]**. Lowering the temperature often leads to a smaller and slower physiological response. Recent studies have demonstrated the efficacy of cooling devices in blocking pain signals in somatic peripheral nerves **[6]**. Extending this concept to the dorsal root ganglia (DRG), which serves as a pivotal point for visceral nociception, may reduce or block pain responses originating from the stomach as shown in **Figure 1**.

To explore this potential therapeutic approach, we propose the development of a micro-liquid thermal regulation device (MLTR) as a non-opioid solution for suppressing visceral gut pain. The fabrication of this device will leverage advancements in 3D printing and microfluidics to achieve targeted cooling. The MLTR will comprise a cooling chip, cooling element, and micro-thermometer. The cooling chip will be microfabricated using digital light processing (DLP) 3D printing, which enables rapid prototyping and iterative testing. The chip will feature a manifold microchannel design, allowing for efficient water flow with minimal pressure **[7]**. The cooling element, an essential component of the MLTR, will establish a closed system. It will utilize Peltier chips in direct contact with a cooling chamber, enabling rapid cooling of the liquid before it reaches the MLTR. This configuration ensures that the device can achieve and maintain low temperatures over an extended period. The micro-thermometer will be attached to the target area to monitor the effectiveness of the cooling process. Our preliminary experiments have demonstrated the MLTR's capability to reach and sustain low temperatures, highlighting its potential as an alternative non-opioid solution for pain management. Integrating 3D printing, microfluidics, and thermoregulation technologies provides a promising avenue for developing this innovative device.

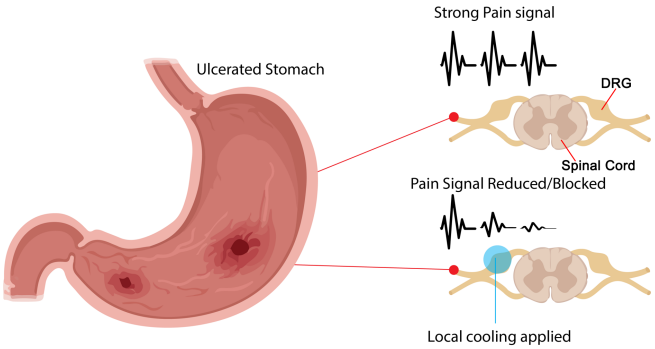

Figure 1. A depiction of an ulcerated stomach. In normal conditions the ulcer will transmit strong pain signals to the central nervous system (CNS) through the dorsal root ganglia (DRG). If local cooling can be applied to the DRG this can reduce the pain signal intensity before it reaches the spinal cord and brain. (Created with Biorender.com).

METHODS

MLTR Design and Fabrication

The MLTR was designed in Autodesk Fusion 360 (USA) into two chips, a bottom microchannel chip and manifold top chip. In **Figure 2A** the top chip dimensions are 3 mm (L) x 3 mm (W) x 1.7 mm (H). The top chip manifold channels themselves consist of two trapezoids that face opposite one another in a 2.4 mm x 2.4 mm square that is extruded to a height of 200 µm. These hollow trapezoids separated by a 200 µm wall, have a depth of 1.5 mm, a shorter lateral side of 300 µm, a longer lateral side of 1 mm, and a length of 2 mm. Finally, a 700 µm diameter inlet/outlet hole is designed on the longer base of the trapezoid. The bottom microchannel chip dimensions are 3 mm (L) x 3 mm (W) x 1.5 mm (H). In the center is a depressed 2.5 mm square which is 200 µm deep designed for integration with the top chip. The four perforated microchannels spaced 258 µm apart from one another, are 2 mm in length, with a width of 300 µm, and placed 200 µm away from the depression walls as shown in **Figure 2B-C**.

The finished design was exported as a .stl file and subsequently imported into the Asiga composer software (Australia). Optimized settings were used for the 3D printing of each chip using an Asiga

978-1-940470-05-4/HH2024/$25©2024TRF
DOI 10.31438/TRF.HH2024.61

Solid-State Sensors, Actuators, and Microsystems Workshop
Hilton Head Island, South Carolina, 2-6 June 2024

Max XUV 27 with Formlabs clear resin (USA). After printing both chips, they were removed from the stage and cleaned using 90% isopropyl alcohol (IPA). Support structures were removed and sanded down until it was flush against the device. The device was then cleaned again by loading it into a 50 ml falcon tube with 90% IPA and inserting it into a sonication bath for 5 minutes and dried. On the top chip a 1/16-inch tubing was adhered onto the inlet and outlet holes using the Formlabs clear resin and spot curing with a handheld UV flashlight. The bottom chip was affixed with a 3 mm x 3 mm square aluminum tape adhered to the flat area with the open microchannels. The aluminum tape was pressed in placed for 5 minutes under a constant pressure of a clamp. The chips were aligned, pressed together, and adhered using the same resin with spot curing with ultra-violet (UV) light. Multiple layers of resin were used to ensure a watertight seal for the device and around the outer area of the aluminum layer (**Figure 3**). Finally, the device was cured in a Formlabs UV chamber for 15 minutes to ensure all resin pieces have been fully cured.

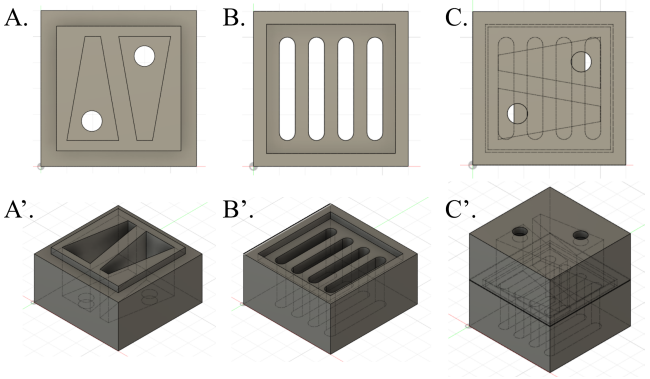

Figure 2. MLTR Schematic Designs. (A) The top design of the MLTR shows the trapezoid manifold design. (A'). 3D side view of the top. (B) The bottom design of the MLTR shows four 300 µm channels that go through the other side. (B'). 3D side view of the bottom. (C) The complete MLTR joins both the bottom and top chips together. The manifold channels run perpendicular to the microchannel. (C'). 3D side view of the complete MLRT.

Cooling unit

The cooling unit of the MLTR comprises various components, including two 12V Peltier chips with heat sinks (Hilitand, USA), Performance Thermal Paste (PTP), fans, a cooling chamber, and heating pipes (Amazon, USA). The PTP (TM30, Corsair, USA) was applied to both sides of the cooling chamber to assemble the core cooling unit. The Peltier chips were then carefully positioned to sandwich the cooling chamber, ensuring that PTP was in contact with the Peltier chip cold surface. The heat sink was then connected to the hot side of the Peltier chips, ensuring proper contact and thermal conductivity. Fans were positioned to facilitate the flow of cold air into one side of the unit while allowing hot air to exit from the other side. (It is important to note that each Peltier device requires its own power source, with one set requiring 120 W and the other requiring 72 W). The ending of a 1/4-inch tubing was then immersed in a 50/50 Antifreeze coolant mixture reservoir and this tubing was then connected to a Masterflex Easy-load 7518 pump allowing the coolant to circulate. Another 1/4 tubing was attached from the pump to the inlet of the cooling chamber. An adapter was used to connect the outlet tubing of the cooling chamber to the inlet tubing of the MLTR. The outlet tubing of the MLTR was then routed back into the reservoir tank creating a closed cooling system, as the coolant was returned to the reservoir.

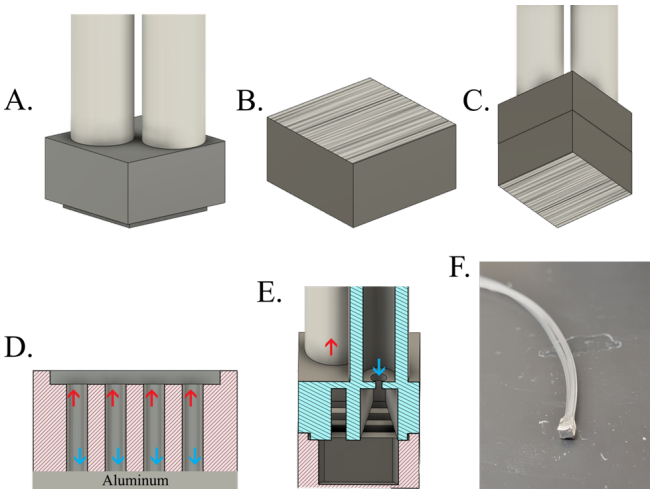

Figure 3. Fabrication and Cross Section Analysis of the MLTR (A) 1/16-inch tubing adhered to the top of the MLTR for both the inlet and outlet openings. (B) An aluminum layer is attached to the bottom piece. (C) 3D design of a completed MLTR with tubing and aluminum layer. (D) Cross section of the bottom piece showing water flow. Cold coolant will cool the aluminum layer before it heats up and leaves through the outlet tubing. (E) Cross section of the complete MLTR. The blue arrow shows the cold inlet, and the red arrow shows the hot outlet for the coolant. (F) Assembled MLTR.

Thermo-regulation testing

To assess the thermo-regulation capabilities of the MLTR, a micro-thermometer was securely attached to the bottom of the device. The thermometer was connected to a controller to enable real-time temperature monitoring. The experiment began by activating the pump to initiate coolant circulation throughout the system. The initial temperature reading was recorded without the MLTR to establish a baseline. Then, the MLTR was installed, and the temperature reading was noted prior to activating the cooling system. Once the cooling system was turned on, temperature measurements were procured at intervals of 30 seconds for a duration of 5 minutes and 10 trials ($n=10$).

Thermo-regulation test on rats

A Sprague Dawley rat (SD male, 9 months) was used to run all the tests. All procedures were carried out under the ethical guidelines of NIH and approved by the Animal Care and Use Committee of University of Central Florida. The MLTR capabilities were then tested on the live rat that was under anesthesia, using isoflurane (#029405, Covetrus, USA) and administered at a 2-3% concentration. The effect of anesthesia was assessed by the absence of the hind paw pinch withdrawal reflex. Once anesthetized the skin, muscle, and DRG were tested using the

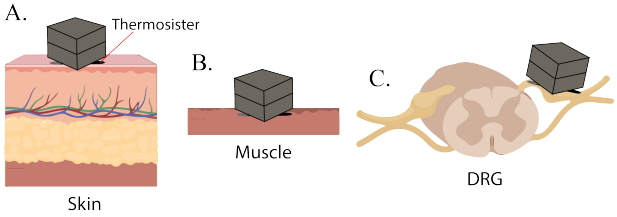

Figure 4. MLTR on rat skin, muscle, and DRG. A. The thermistor is placed between the skin and the MLTR. B. The muscle was exposed, and the thermistor was placed between it and the MLTR. C. The DRG was exposed, and the thermistor was placed between it and the MLTR. (Created with Biorender.com).

MLTR as shown in **Figure 4**. The temperature readings were obtained by placing a thermistor, which was connected to a temperature reader (as described in the thermo-regulation testing section), between the MLTR and the area of interest. The basal temperature was obtained for each area while the device was turned off, then the device was turned on and a temperature reading was obtained at every 30 seconds for a duration of 5 minutes. This test was repeated for the skin, muscle, and DRG region for a total of 300 seconds and 6 trials (*n=6*).

RESULTS

3D Printed MLTR Microfabrication

The precision of the 3D print is crucial when being able to replicate the design dimensions as described in the methods section MLTR design and fabrication. The dimensions of the hole shown in

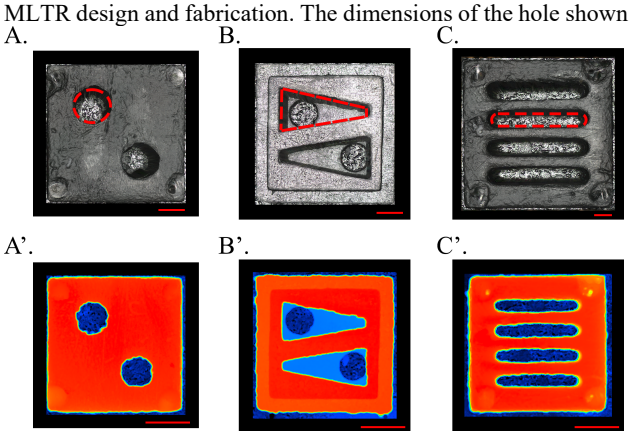

Figure 5. Confocal imaging of the 3D printed MLTR in A, B, and C. A', B', C' are height images of the MLTR. Scale Bars for (A) and (B) are 400 µm, (C) is 300 µm and (A'), (B'), (C') is 1000 µm.

Figure 5A are an average of 611.88 µm, resulting in a **3.2 %** error from the design dimensions. The trapezoid shown in **Figure 5B** has an area of 1.19 mm^2 resulting in an **8.46% error**. The printed microchannels measured an average of 260.26 µm, which represents a **13.25% error**. These effective miniscule tolerances seamlessly allowed for the viability of the chips to integrate with one another for further characterization.

MLTR Temperature test

The effectiveness of the thermal regulation device is demonstrated in **Figure 6.** A PerfectPrime thermal camera with an emissivity of 0.95 was used on the MLTR under room temperature, showing that the **coldest surface of the device was 13.8°C**. The experiments were conducted over 300 seconds, with temperature measurements obtained at 30-second intervals. The initial temperature recorded before activating the MLTR was 23.88°C on average. The temperature gradually decreased throughout the **300-second trial period, reaching an average temperature of 15.48°C**. This corresponds to an **average temperature drop of 8.4°C** as shown in **Figure 6**. The lowest temperature achieved in the **5-min test was 14.5°C**, 9.3°C below room temperature.

MLTR thermoregulation test on a rat

The temperature test on the rats were performed on 3 regions which were the skin, muscle, and DRG. In the ***skin***, the temperature was reduced from **average basal temperature (33.65 °C) to an average of 27.32 °C**. In the **exposed muscle**, the temperature was reduced from **average basal temperature (33.95 °C) to an average of 25.85 °C.** In the **DRG**, the temperature was reduced from **average basal temperature (35.58 °C) to 26.3 °C**. The average temperature change brought by the MLTR to the skin, muscle, and **DRG was 6.3 °C, 8.1 °C, and 9.3 °C**, respectively as shown in **Figure 7**.

DISCUSSION

The MLTR presents a promising alternative to opioid-based therapies for managing chronic visceral gut pain. Its ability to achieve temperatures lower than the physiological norm of 37°C suggests the potential to influence the underlying physiological

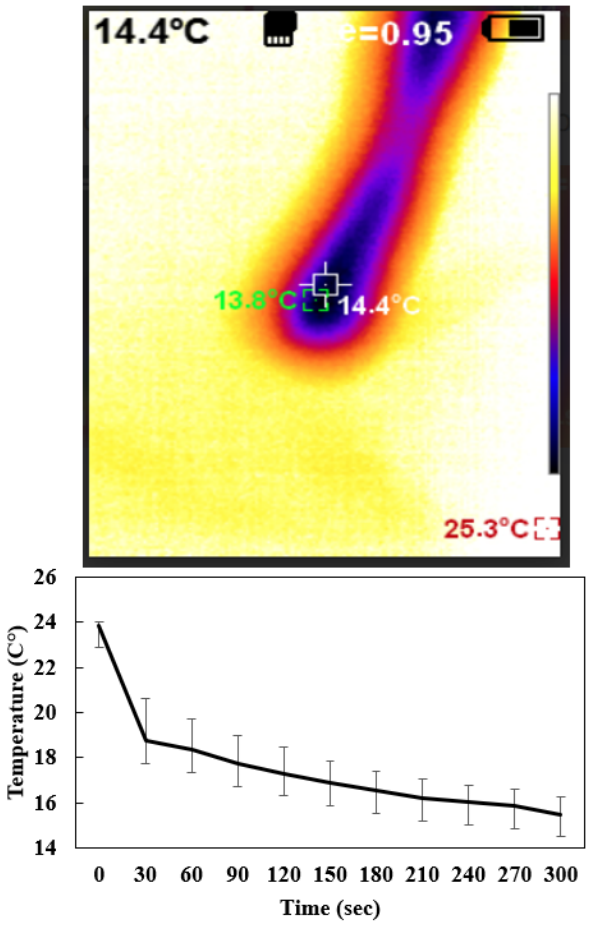

Figure 6. Thermal Image and graph of the average temperature change in room temperature of the MLTR. (Top) Thermal image shows internal temperature of 13.8°C indicated by the dark blue color, outside temperature of 14.4°C indicated at the boundary of the purple and red area as well as a room temperature of 25.3°C indicated in the white color. (Bottom) The MLTR was utilized in a room temperature setting during the trials (n=10 trials) to assess its cooling capability.

processes associated with pain transmission. An outstanding feature of the MLTR is its compact design, making it feasible for implantation into the DRG to assess its impact on pain signaling to the brain. We have also demonstrated that implantation of the MLTR onto the DRG was able to lower the local temperature to 26.3 °C. While previous research has demonstrated the effectiveness of cooling in blocking pain signals **[6]**, the MLTR distinguishes itself by integrating 3D printing technology and a closed-loop cooling system. The closed-loop cooling mechanism of the MLTR holds the potential for portability, further enhancing its practicality for pain management applications.

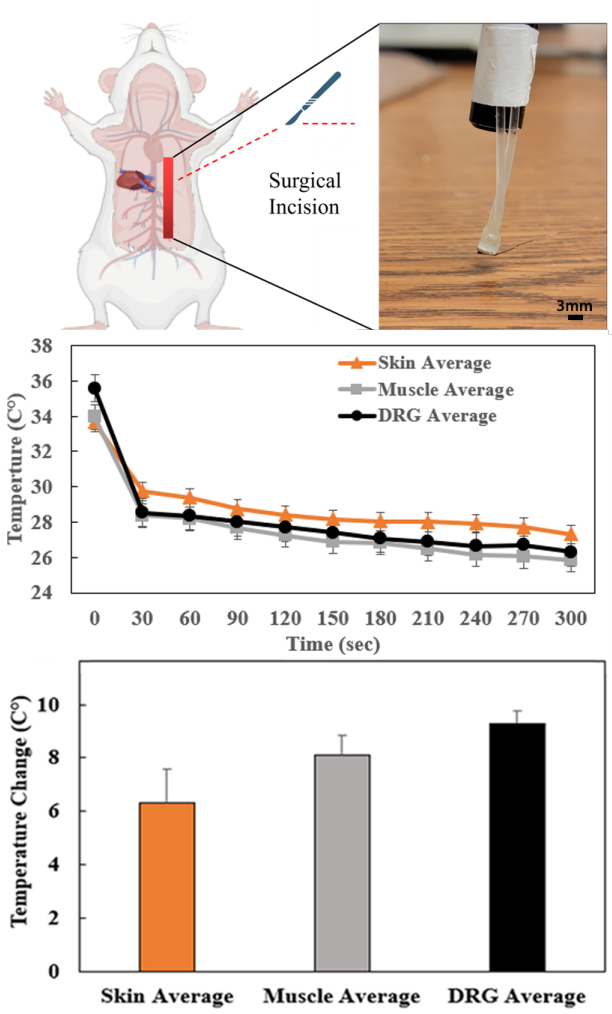

Figure 7. Surgical incision area of Micro Liquid Thermal Regulator along the spinal cord of the rat, showing the crucial portion of the central nervous system. (Right) Showing the complete construction of MLTR with the cooling outlet. As well as the total temperature change of the skin, muscle, and dorsal root ganglion average (n=6 trials). (Created with Biorender.com).

In our real-world testing, the MLTR demonstrated its effectiveness by lowing baseline temperature in specific locations such as the skin, muscle, and dorsal root ganglia. We significantly reduced the DRG's localized temperature to 26.3°C, demonstrating the MLTR's potential for targeted therapeutic cooling. However, various challenges must be addressed before the MLTR can be used in a therapeutic setting. A primary concern is the development of a non-toxic, thermally conductive glue that can securely attach the MLTR to the targeted locations while causing no harm **[8]**, Furthermore, developing a method to reliably detect pain levels in rats after induced visceral gut pain is vital to test its efficiency. The future development of the MLTR itself will take shape in phases. The first phase would primarily involve increasing the cooling efficiency by exploring bio-compatible and thermally conductive material for the MLTR. It also examines the efficiency of the liquid. The second phase would be implanting multiple MLTR on all the DRG from T7-T11 which conveys the nociceptive singles from the stomach to the CNS of the rat **[9, 10]**. Blocking multiple DRG sites would allow for a more significant effect of reducing or even halting the pain signals from the stomach reaching the CNS. At this stage, we will run a pain test on the rats by inducing gut pain while they are under anesthesia to see the compounding effects of multiple MLTRs. The final phase would be to test the MLTR on awake rats and observe how the rats adapt to the implant.

The MLTR stands out as a novel non-opioid pain treatment strategy for chronic visceral gut pain. Its design integrates 3D printing and a closed-loop cooling system, which increases its versatility, cost-effectiveness, and customizability. These characteristics make the MLTR a promising choice for future study and development aimed at improving non-opioid pain treatments. Continued research and development of the MLTR are required to meet the pressing demand for safe and effective non-opioid therapies for visceral gut pain. The advancement in this field offers hope for significant advances in pain management tactics.

Acknowledgements

This work was supported by a grant from NIH HEAL Initiative (The Helping to End Addiction Long-term® Initiative; https://heal.nih.gov/): NIH U01 NS113867-01 (ZJC) and UCF RF funding and UCF MSE GTA for Andre Childs. We would also like to thank Hilton Head 2024 for travel funding to attend the meeting.

REFERENCES

[1] C. E. Zelaya, J. M. Dahlhamer, J. W. Lucas, and E. M. Connor, "Chronic Pain and High-impact Chronic Pain Among U.S. Adults, 2019," NCHS Data Brief, no. 390, pp. 1–8, Nov. 2020.

[2] L. A. Trachsel, S. Munakomi, and M. Cascella, "Pain Theory," in StatPearls, Treasure Island (FL): StatPearls Publishing, 2024. Accessed: Apr. 12, 2024. [Online]. Available: http://www.ncbi.nlm.nih.gov/books/NBK545194/

[3] B. Greenwood-Van Meerveld and A. C. Johnson, "Mechanisms of Stress-induced Visceral Pain," J Neurogastroenterol Motil, vol. 24, no. 1, pp. 7–18, Jan. 2018, doi: 10.5056/jnm17137.

[4] D. Cantarero-Prieto and P. Moreno-Mencia, "The effects of gastrointestinal disturbances on the onset of depression and anxiety," PLoS One, vol. 17, no. 1, p. e0262712, Jan. 2022, doi: 10.1371/journal.pone.0262712.

[5] P. Sosnowski, K. Mikrut, and H. Krauss, "[Hypothermia--mechanism of action and pathophysiological changes in the human body]," Postepy Hig Med Dosw (Online), vol. 69, pp. 69–79, Jan. 2015, doi: 10.5604/17322693.1136382.

[6] J. T. Reeder et al., "Soft, bioresorbable coolers for reversible conduction block of peripheral nerves," Science, vol. 377, no. 6601, pp. 109–115, Jul. 2022, doi: 10.1126/science.abl8532.

[7] D. Kong et al., "A holistic approach to thermal-hydraulic design of 3D manifold microchannel heat sinks for energy-efficient cooling," Case Studies in Thermal Engineering, vol. 28, p. 101583, Dec. 2021, doi: 10.1016/j.csite.2021.101583.

[8] G. Bovone, O. Y. Dudaryeva, B. Marco-Dufort, and M. W. Tibbitt, "Engineering Hydrogel Adhesion for Biomedical Applications via Chemical Design of the Junction," ACS Biomater. Sci. Eng., vol. 7, no. 9, pp. 4048–4076, Sep. 2021, doi: 10.1021/acsbiomaterials.0c01677.

[9] J. Ma et al., "Spinal afferent innervation in flat-mounts of the rat stomach: anterograde tracing," Sci Rep, vol. 13, no. 1, p. 17675, Oct. 2023, doi: 10.1038/s41598-023-43120-y.

[10] J. Ma et al., "Organization and morphology of calcitonin gene-related peptide-immunoreactive axons in the whole mouse stomach," J Comp Neurol, vol. 531, no. 16, pp. 1608–1632, Nov. 2023, doi: 10.1002/cne.25519.

CONTACT

Zixi Cheng, tel: +1-321-331-3871; Zixi.Cheng@ucf.edu